Eur Biophys J
DOI 10.1007/s00249-017-1243-5

ORIGINAL ARTICLE

EBSA
Biophysics in Europe

# Conformational changes, from β-strand to α-helix, of the fatty acid-binding protein ReP1-NCXSQ in anionic lipid membranes: dependence with the vesicle curvature

**Vanesa V. Galassi[1,2,3] · Silvina R. Salinas[1,2,4] · Guillermo G. Montich[1,2]**

Received: 23 March 2017 / Revised: 31 May 2017 / Accepted: 10 July 2017


**Abstract** We studied the conformational changes of the fatty acid-binding protein ReP1-NCXSQ in the interface of anionic lipid membranes. ReP1-NCXSQ is an acidic protein that regulates the activity of the $Na^+/Ca^{2+}$ exchanger in squid axon. The structure is a flattened barrel composed of two orthogonal β-sheets delimiting an inner cavity and a domain of two α-helix segments arranged as a hairpin. FTIR and CD spectroscopy showed that the interactions with several anionic lipids in the form of small unilamellar vesicles (SUVs) induced an increase in the proportion of helix secondary structure. Lower amount or no increase in α-helix was observed upon the interaction with anionic lipids in the form of large unilamellar vesicles (LUVs). The exception was 1,2-dimyristoyl-*sn*-glycero-3-phosphoglycerol (DMPG) that was equally efficien to to induce the conformational change both in SUVs and in LUVs. In solution, the infrared spectra of ReP1-NCXSQ at temperatures above the unfolding displayed a band at 1617 $cm^{-1}$ characteristic of aggregated strands. This band was not observed when the protein interacted with DMPG, indicating inhibition of aggregation in the interface. Similarly to the observed in L-BABP, another member of the fatty acid binding proteins, a conformational change in ReP1-NCXSQ was coupled to the gel to liquid-crystalline lipid phase transition.

**Keywords** ReP1-NCXSQ · Lipid membrane · Protein conformational change · Infrared spectroscopy · Circular dichroism · Membrane curvature

**Abbreviations**

| | |
|---|---|
| ReP1-NCXSQ | Regulatory protein of the squid nerve sodium calcium exchanger |
| FABP | Fatty acid-binding protein |
| L-BABP | Chicken liver bile acid-binding protein |
| DMPG | 1,2-dimyristoyl-*sn*-glycero-3-phosphoglycerol |
| DPPG | 1,2-dipalmytoyl-*sn*-glycero-3-phosphoglycerol |
| POPG | 1-palmitoyl-2-oleoyl-*sn*-glycero-3-phosphoglycerol |
| DMPA | 1,2-dimyristoyl-*sn*-glycero-3-phosphate |
| DMPS | 1,2-dimyristoyl-*sn*-glycero-3-phosphoserine |
| DPPA | 1,2-dipalmitoyl -*sn*-glycero-3-phosphate |
| DLPA | 1,2-dilauroyl-*sn*-glycero-3-phosphate |
| DMPC | 1,2-dimyristoyl-*sn*-glycero-3-phosphocholine |
| LUV | Large unilamellar vesicle |
| FTIR | Fourier transform infrared |
| CD | Circular dichroism |
| FSD | Fourier self-deconvolution |

Vanesa V. Galassi and Silvina R. Salinas contributed equally to the work.

✉ Guillermo G. Montich
gmontich@fcq.unc.edu.ar

[1] Departamento de Química Biológica "Ranwel Caputto", Facultad de Ciencias Químicas, Universidad Nacional de Córdoba, Córdoba, Argentina

[2] Centro de Investigaciones en Química Biológica de Córdoba (CIQUIBIC), CONICET, Universidad Nacional de Córdoba, Córdoba, Argentina

[3] Present Address: CONICET, Facultad de Ciencias Exactas y Naturales, Universidad Nacional de Cuyo, M5502JMA Mendoza , Argentina

[4] Present Address: Centro de Excelencia en Productos y Procesos Córdoba-CONICET, Pabellón CEPROCOR, X5164, Santa María de Punilla, Córdoba, Argentina

Published online: 27 July 2017

## Introduction

The association of soluble proteins with lipid membranes is coupled to conformational changes of the protein and rearrangement of the membrane. These changes can modulate the biological activity of the protein and trigger relevant processes in the cell physiology. For example, lipolytic enzymes are activated within the membrane environment (Ramirez and Jain 1991; Berg et al. 2001; Verger 1997; Fanani et al. 2010; Cornell and Ridgway 2015), the self-aggregation of proteins related to several diseases can be induced by membrane interactions (Gorbenko and Trusova 2011), fatty acid binding proteins translocate from the aqueous media to the lipid membrane and transfer non-polar solutes between cell membranes as a key step in several physiological processes (Storch and McDermott 2009). The modifications induced in the protein include changes in secondary and tertiary structure, peptides like melittin (Drake and Hider 1979; Fidelio et al. 1982) or proteins like synuclein (Perrin et al. 2000) and phosphocholine cytidylyltransferase (Cornell and Ridgway 2015), with fluctuating, unordered structure in solution, acquire defined secondary structure when they bind to the lipid membrane; on the other side, proteins with well-defined secondary structure in solution like β-lactoglobulin (Lefèvre and Subirade 2001; Zhang and Keiderling 2006), prothrombin (Wu and Lentz 1991), β2-human glycoprotein (Wang et al. 2000; Paolorossi and Montich 2011) can undergo strand-to-helix transition in the lipid membrane interface. Besides explaining the relationship of these changes with the mechanisms of cell process, it is interesting to use these systems to understand how the anisotropic environment of the interface imposes different rules for the folding process as compared with the isotropic aqueous solution.

In this work, we describe the conformational changes of the protein ReP1-NCXSQ in anionic lipid membrane. ReP1-NCXSQ is an acidic protein that regulates the activity of the $Na^+/Ca^{2+}$ exchanger in squid axon (Berberián et al. 2009, 2012; Raimunda et al. 2009; Cousido-Siah et al. 2012). ReP1-NCXSQ belongs to the family of the cellular retinoic acid-binding proteins, CRABPs, and to the superfamily of the fatty acid-binding proteins, FABPs. The structure is a flattened barrel composed of two orthogonal β-sheets delimiting an inner cavity and a domain of two α-helix segments arranged as a hairpin (PDB ID: 3PP6, Cousido-Siah et al. 2012). We previously described that ReP1-NCXSQ binds preferentially to anionic lipid membranes acquiring an orientation in the interface determined by its interactions with the membrane local electric field (Galassi et al. 2014). We found that other member of the FABP family, the basic liver bile acid binding protein, L-BABP, binds to anionic lipid membranes and acquires a partially unfolded state with an increase in the proportion of α-helix secondary structure (Nolan et al. 2003). The structural rearrangements are coupled to the changes in the membrane electrostatic surface potential, which at its time are determined by the lipid phase state (Decca et al. 2007, 2010). Similarly, in the present work, we show that ReP1-NCXSQ was bound to anionic lipid membrane and increased the amount of α-helix, with a conformational change coupled to the lipid phase transition and the curvature of the lipid membrane. As a difference with L-BABP, the interaction with the anionic lipid DMPG inhibits the protein self-aggregation at high temperatures. We also show that the membrane curvature influences on the proportion of α-helix increase upon lipid-membrane binding.

Our main interest was to use ReP1-NCXSQ as a model system to study general aspects about the interactions of proteins with lipid membranes, but at the same time our results can be useful to understand the activation of the $Na^+/Ca^{2+}$ transporter by ReP1-NCXSQ.

## Materials and methods

ReP1-NCXSQ cDNA was synthesized and codon-optimized for *Escherichia coli*. 1,2-dimyristoyl-*sn*-glycero-3-phosphoglycerol (DMPG), 1,2-dipalmytoyl-*sn*-glycero-3-phosphoglycerol (DPPG), 1-palmitoyl-2-oleoyl-*sn*-glycero-3-phosphoglycerol (POPG), 1,2-dimyristoyl-*sn*-glycero-3-phosphate (DMPA), 1,2-dimyristoyl-*sn*-glycero-3-phosphate (DMPA), 1,2-dimyristoyl-*sn*-glycero-3-phosphoserine (DMPS), 1,2-dimyristoyl-*sn*-glycero-3-phosphocholine (DMPC), 1,2-dipalmitoyl -*sn*-glycero-3-phosphate (DPPA) 1,2-dilauroyl-*sn*-glycero-3-phosphate (DLPA) were from Avanti Polar Lipids (Alabaster, AL, USA). $^2H_2O$ 99.9+% was supplied by Nucleoeléctrica Argentina S.A. Central Nuclear Embalse, Div. Química y Procesos.

### Expression and purification of ReP1-NCXSQ

The cDNA for ReP1-NCXSQ was cloned into the expression vector pGEX4T2 and expressed in *Escherichia coli* strain BL21. The fusion protein GST-ReP1-NCXSQ was purified by affinity chromatography in glutathione-Sepharose resin and eluted with reduced glutathione. GST-ReP1-NCXSQ was cleaved with thrombin and ReP1-NCXSQ was purified by exclusion chromatography in Superdex 75. While the expression yield of the fusion protein was acceptable, the cleavage with thrombin was a very inefficient step. The final yield of ReP1-NCXSQ was 0.3 mg of pure protein per liter of starting culture medium. The ReP1-NCXSQ preparation produced a single band with an apparent MW = 15 kDa in SDS-PAGE. The protein was quantified by the absorbance at 280 nm using $\varepsilon_{280} = 14{,}000\ M^{-1}cm^{-1}$.

### Large unilamellar vesicles preparation

Large unilamellar vesicles (LUVs) were prepared as in Nolan et al. (2003). Pure phospholipids were dissolved in chloroform:methanol 2:1 vol:vol, dried with a stream of $N_2$ to form a thin film in a glass tube and placed under vacuum to remove traces of organic solvent. The dry lipids were hydrated with aqueous solutions containing 0.01 or 0.1 M NaCl. After five cycles of freezing in liquid nitrogen and thawing at 60 °C, LUVs were prepared by ten cycles of extrusion through polycarbonate filters with pores of 100 nm. Dynamic light scattering measurements showed that the vesicles were of 96 ± 7 nm diameter. For the FTIR experiments we prepared the LUVs in $^2H_2O$.

### Small unilamellar vesicles preparation

The lipids hydrated in 0.01 or 0.1 M NaCl as in the preparation for LUVs were vigorously shaken in a vortex and placed in a tip sonifier surrounded by a water bath at room temperature in a $N_2$ atmosphere. Samples were sonified in several pulses for a total time of 2 min until the turbidity largely decreased. Debris of the titanium tip was removed in a bench centrifuge. Dynamic light scattering were performed in a particle sizer Nicomp 380 and revealed a monodispersed preparation with sizes between 20 and 40 nm diameter depending on the particular lipid.

### Binding filtration assay

Lipid-protein mixtures were loaded in the upper chamber of Microcon YM100 concentrators (Amicon) and spun down at 7500×*g* until 80% of the initial volume was eluted. The amount of protein in the initial sample and in the eluate were evaluated by the absorbance at 280 nm.

### FTIR spectroscopy

The protein was lyophilized from aqueous solution, dissolved in $^2H_2O$, and incubated overnight at room temperature to allow deuterium exchange of the amide protons. LUVs and pure protein were allowed to equilibrate at 10–15 °C for 15 min before mixing the solutions and then transferred to a cell equilibrated at the initial temperature. Spectra were recorded in a Nicolet Nexus spectrometer using a thermostated demountable cell for liquid samples with $CaF_2$ windows and 75 μm Teflon spacers. The spectrometer was flushed with dry air to reduce water vapor distortions in the spectra. Normally, 50 scans were collected both for the background and the sample at a nominal resolution of 2 $cm^{-1}$. The temperature in the cell was controlled with a circulating water bath. The temperature setting in the bath was manually increased in steps of 5 °C. The actual temperature in the sample, measured with a calibrated thermocouple inserted in the cell, increased continuously with a rate of about 0.5 °C/min. The acquisition of a spectrum at a given nominal temperature (that is, the acquisition of the 50 individual scans) lasted 1 min and spanned a change in the temperature of about 0.5 °C. Data plotted in Fig. 2 correspond to the temperature readings in the midpoint of that segment of time. The contribution of the $^2H_2O$ in the amide I′ region was eliminated by subtracting the absorbance of $^2H_2O$ acquired at the corresponding temperature. A linear baseline was defined between 1600 and 1700 $cm^{-1}$ and the area was normalized to unity between these limits. The FTIR measurements as a function of the temperature were repeated in three separate samples for each system. Data acquisition and Fourier self-deconvolution (FSD) of the spectra was performed with the Omnic software supplied by Nicolet. In principle, a large number of combinations of area, bandwidth, and location of the band components can suitably adjust to an experimental spectrum yielding an artefactual proportion of secondary structure components. To obtain a realistic representation of the protein structure, we followed the procedure used by Arrondo and Goñi (1999). In brief, once the component bands were identified by FSD and second derivative, we performed the fitting iteratively allowing to vary only one parameter (integral area, bandwidth, and band location) at a time and within a narrow range of values. In this way, a proportion of secondary structure components in fair agreement with the crystallographic structure can be obtained.

### Circular dichroism

The measurements were made with a Jasco J-810 spectropolarimeter using a 0.2-cm path length quartz cell. Each spectrum was an average of six scans. The protein concentration was 10 μM. The contribution of the buffer was subtracted in all spectra. Scan speed was set to 50 nm/min, with a response time of 2 s, a data pitch of 0.2 nm, and a bandwidth of 2 nm. The temperature was measured with a calibrated thermocouple in contact with the sample. The rate of temperature increase was similar to the FTIR experiments. The contribution of secondary structure components was evaluated with the programs CONTINLL (Provencher and Glöckner 1981), SELCON (Sreerama and Woody 1993, 2000) and CDSSTR (Johnson 1999), using the tools supplied by CDPro software package (Provencher and Glöckner 1981). CONTINLL, SELCON, and CDSSTR evaluate the proportion of helix, β-strand, turns, and unordered structures by comparing the experimental spectrum with a set of representative proteins of known crystallographic structure and unfolded proteins. Each program calculates the proportions of secondary structure using a particular algorithm and independently of the others (Provencher and

Glöckner 1981). In this work, we used the average value of the three outputs. Each output always differed in less than 5% of the average. To calculate $\Delta\varepsilon$ from the ellipticity values, we used 133 residues per protein molecule.

## Results

We used FTIR and CD spectroscopy to study the conformational changes of RePl-NCXSQ in LUVs of DMPG and DOPG as a function of the temperature. We also used CD spectroscopy to study the interactions with vesicles of anionic lipids with different curvature: extruded LUVs and sonicated SUVs.

As described in the "Materials and methods" section, we expressed the native sequence of RePl-NCXSQ without the histidine tag used for purification. FTIR and CD spectra of this molecule were identical to the labeled protein used in previous work (Berberián et al. 2009).

When expressed in bacteria, proteins that bind nonpolar or amphiphilic compounds spontaneously incorporate ligands taken from the host cell, which are not necessarily the same ligands taken and operating in the native environment (De Gerónimo et al. 2010; Rey-Burusco et al. 2015; Micheletto et al. 2017). The crystallographic structure of RePl-NCXSQ expressed in *E. coli* revealed a palmitoleic acid located in the inner cavity. The protein purified from squid, instead, contains a palmitic acid (Cousido-Siah et al. 2012). For the present studies, we used the protein as purified from the expression system without delipidation or ligand substitution, this contains palmitoleic acid.

### FTIR spectroscopy

#### *Influence of the protein on the lipid phase transition*

We have not detected changes in the thermal behavior of LUVs of DMPG in the presence of Rep1-NCXSQ according to FTIR spectroscopy. The position of the bands between 2890 and 2850 $cm^{-1}$ due to $–CH_2–$ stretching and the ratio between the two bands at 1731 and at 1742 $cm^{-1}$ due to the carbonyl group in phospholipids are sensitive to the lipid phase state (Casal and Mantsch 1984). Both parameters, band position and band ratio, displayed a sharp sigmoidal change with a midpoint at 24 °C for DMPG (Decca et al. 2007, 2010). No changes in the transition curves were observed in the presence of RePl-NCXSQ, suggesting that the protein did not influence on the lipid structure and cooperativity of the transition (results not shown). Nevertheless, it must be taken into account that the experiments were performed in the presence of saturating amounts of lipid. Then, it cannot be discarded that the protein produced a local reorganization of the lipids.

#### *RePl-NCXSQ conformations*

Figure 1 shows the infrared spectra of the protein in solution and in the presence of lipids at 20 and at 60 °C. In solution, at 20 °C, the spectrum showed a large proportion of β structure. FSD and second derivative of the deconvoluted spectrum revealed bands at 1627, 1637, and 1671 $cm^{-1}$ assigned to β strands, at 1652 $cm^{-1}$ assigned to α-helix and at 1684 $cm^{-1}$ assigned to β turns (Byler and Susi 1986). The areas of the bands that best fit the experimental spectrum can be considered proportional to the assigned structures. Table 1 shows the band proportion. We obtained 70% of β structure (35.8 + 26.1 + 8.6 in Table 1), and 17% of α helix for native RePl-NCXSQ at 20 °C in solution (see comparison with DSSP analysis and CD measurements in the discussion). A large change in the spectrum at 20 °C was observed in the presence of LUVs of DMPG at low ionic strength (0.01 M NaCl, Fig. 1). The peaks were less defined and little structure was observed in the experimental spectrum. FSD and second derivative revealed bands at about the same location as in the native protein in solution (Fig. 1a) except for the band at 1637 $cm^{-1}$. This band was not evident as a neat minimum in the second derivative, but it was necessary to include it arbitrarily to obtain an acceptable fitting. The area of the band at 1627 $cm^{-1}$, corresponding to β-strands, (shifted to 1624 $cm^{-1}$ after fitting) decreased from 35.6% in solution to 19.3% (Table 1). A new band with 16% of the area, assigned to unordered structure, appeared at 1645 $cm^{-1}$. Remarkably, the area of the band at 1652/1654 $cm^{-1}$ increased from 17.4% in solution to 23.2%, indicating a proportional increase in α-helix (Table 1). Increasing the ionic strength to 0.1 M NaCl produced a state with intermediate characteristics between the protein in solution and in the presence of DMPG at low ionic strength. The spectra displayed a native-like shape, but the bands were also less defined. The amount of β-strands decreased, unordered structure (band near 1645 $cm^{-1}$) was not present and α-helix structure also increased as compared with the protein in solution (band at 1653 $cm^{-1}$, 25% of the area, in Table 1).

In the presence of POPG at 20 °C, the bands revealed by second derivative of FSD spectra and their proportions were similar to the protein in solution.

At 60 °C in solution (above the unfolding temperature, see next section), the dominant bands were at 1617 and 1683 $cm^{-1}$, corresponding to aggregated structure. In the presence of DMPG and 0.01 M NaCl, a condition of relative strong interaction with the anionic lipid membrane, some secondary structure was retained as compared with 20 °C and remarkably no bands of aggregation were observed. Decreasing the electrostatic interactions by increasing the ionic strength to 0.1 M NaCl RePl-NCXSQ was aggregated in the presence of DMPG. In POPG, low ionic strength, we

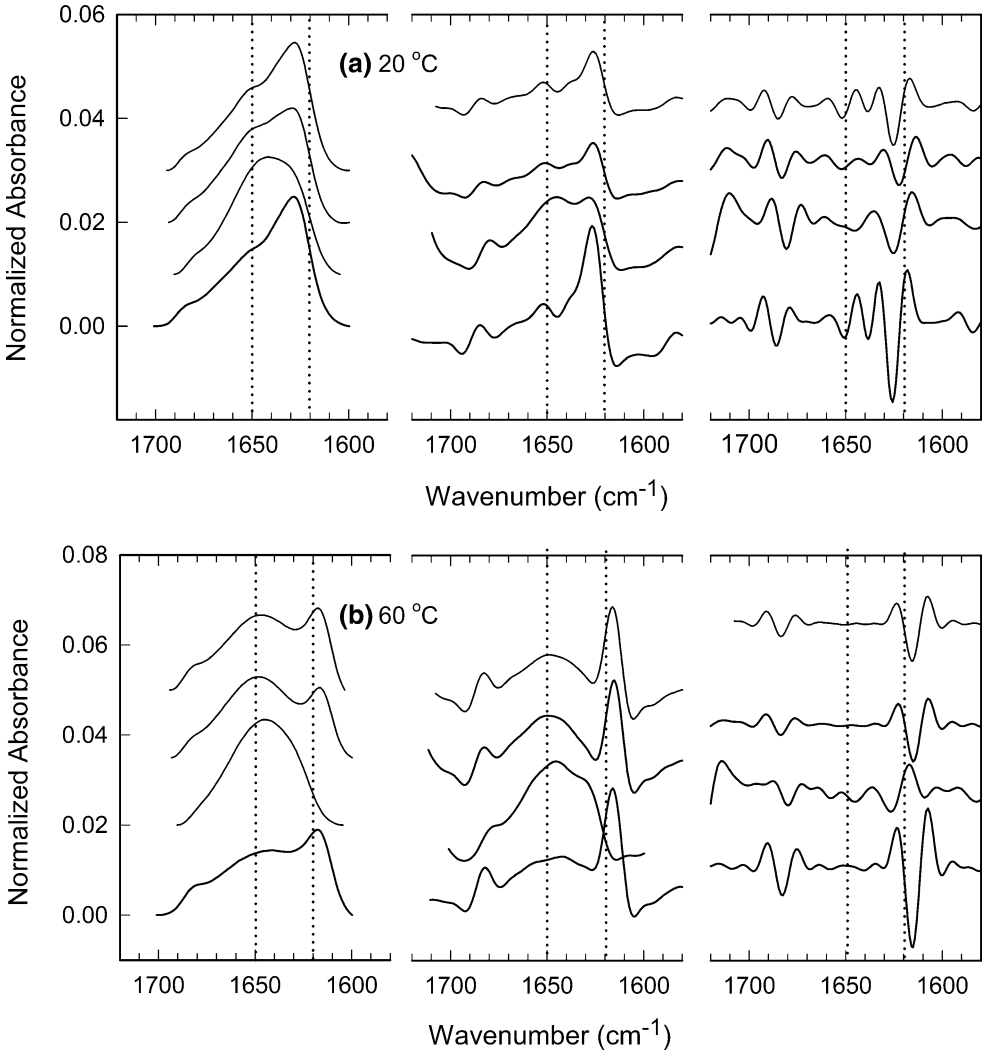


**Fig. 1** FTIR spectra of RePl-NCXSQ. **a** Spectra obtained at 20 °C. **b** Spectra obtained at 60 °C. *Left panels* experimental spectra. *Middle panels* deconvoluted spectra using $k = 2$ and FWHH = 18 $cm^{-1}$. *Right panels* second derivative of the deconvoluted spectra. In all panels from bottom to top, RePl-NCXSQ in solution 0.01 M NaCl; RePl-NCXSQ with DMPG 0.01 M NaCl; RePl-NCXSQ with DMPG 0.1 M NaCl, RePl-NCXSQ with POPG 0.01 M NaCl. Concentrations were 130 μM protein and 13 mM lipid. pD 6.1. *Dotted lines* are drawn as a guide at 1620 and 1650 $cm^{-1}$

also observed bands of aggregation, suggesting a weaker interaction with this lipid as compared with DMPG.

*Temperature dependence of the spectra*

Figure 2 shows the dependence of the spectral shape as a function of the temperature. The spectra were normalized to unit area between 1600 and 1700 $cm^{-1}$. The absorbance at selected wavenumbers of the normalized spectra can be used as a representative parameter of the spectral shape. We used the absorbance at 1627 $cm^{-1}$ (band corresponding to β structure, filled circles) and at 1617 $cm^{-1}$ (band corresponding to aggregates, empty circles). In solution (Fig. 2a), a small, continuous change was observed within the range 18–40 °C. Within the temperature range 40–50 °C, the band at 1627 $cm^{-1}$ decreased in a sigmoidal way. Together with the decrease in β-strands, a new band at 1617 $cm^{-1}$, assigned to aggregated extended structures (Surewicz et al. 1990), increased as a function of the temperature. Figure 1 shows the spectrum acquired above the unfolding temperature. Bands corresponding to β-strands or α-helix were less defined than at low temperature, while the band of unordered aggregated structure was neatly observed at 1617 $cm^{-1}$ (see Fig. 1b, lower traces).

In the presence of DMPG LUVs, 0.01 M NaCl, the shape of the spectra remained constant along the whole temperature range and only displayed a continuous and small decrease in the absorbance at 1627 $cm^{-1}$ (Fig. 2b) with a concomitant increase in the absorbance at 1650 $cm^{-1}$ (not shown). Remarkably, no aggregation (as revealed by the band at 1617 $cm^{-1}$) was present even at the highest temperatures.

In the samples containing LUVs of DMPG and 0.1 M NaCl (Fig. 2c), we observed two transitions as a function of the temperature for RePl-NCXSQ. The normalized absorbance at 1627 $cm^{-1}$ decreased within the range 20–30 °C. This temperature range is coincident with the transition of DMPG from the gel to the intermediate phase (see below), which is centered at 24 °C. We have also observed this behavior for the fatty acid binding protein L-BABP (Decca

**Table 1** Band components of the FTIR spectra of ReP1-NCXSQ in solution and in the presence of lipids

| ReP1-NCXSQ in solution | | ReP1-NCXSQ DMPG 0.01 M NaCl | | ReP1-NCXSQ DMPG 0.1 M NaCl | |
|---|---|---|---|---|---|
| Position[a] $cm^{-1}$ | % of area | Position[a] $cm^{-1}$ | % of the area[b] | Position[a] $cm^{-1}$ | % of the area[b] |
| 20 °C | | | | | |
| 1626 | 36 ± 4 | 1624 | 19 ± 2 | 1626 | 30 ± 0.7 |
| 1638 | 26 ± 1 | 1635 | 27 ± 1 | 1639 | 28 ± 1.4 |
| | | 1645 | 16 ± 0.4 | | |
| 1652 | 17 ± 0.6 | 1654 | 23 ± 0.7 | 1653 | 25 ± 1.4 |
| 1661 | 8 ± 2.4 | 1667 | 12 ± 2 | 1669 | 17 ± 1.4 |
| 1671 | 9 ± 0.23 | | | | |
| 1684 | 3.8 ± 2 | 1680 | 2 ± 1 | 1683 | 2 ± 1 |
| 34 °C | | | | | |
| 1626 | 33 ± 1 | 1627 | 20 ± 0.7 | 1623 | 15 ± 0 |
| 1638 | 26 ± 0.6 | 1635 | 19 ± 2.8 | 1637 | 33 ± 0 |
| | | 1645 | 28 ± 0.7 | | |
| 1652 | 19 ± 0.6 | 1657 | 22 ± 0.7 | 1652 | 32 ± 0.5 |
| 1661 | 8 ± 0.7 | 1669 | 9 ± 1.4 | 1667 | 17 ± 0.5 |
| 1671 | 9 ± 0.6 | 1676 | 2 ± 0 | | |
| 1684 | 4 ± 0.5 | | | 1681 | 2.5 ± 0 |

Band components were fitted to the normal, not deconvolved spectra of the amide I' absorption of ReP1-NSβ2GPI in solution. Data correspond to the plots in Fig. 1

[a] Band position after fitting procedure

[b] Percentage of the area of the amide band, *numbers* are the average of three separate samples for the protein in solution and two separate samples in the presence of lipid ±SD

et al. 2007, 2010). Table 1 shows the composition of secondary structure above this first transition, at 34 °C. A remarkable feature was the increase from 25 to 32% in the proportion of α-helix. A second transition within the range of 40–50 °C, coincident with the main thermal unfolding transition for the protein in solution, produced a protein in a state similar to that observed in the absence of lipids: the secondary structure decreased and the unordered aggregated structure (band at 1617 $cm^{-1}$) was increased.

In the presence of the anionic lipid POPG, 0.01 M NaCl, a single transition was observed, also leading the protein to an aggregated state, as shown by the increase in the band at 1617 $cm^{-1}$ (Fig. 2d). This transition, with a midpoint at 43 °C, occurred 5° below the transition of the pure protein. This suggests that, even when the spectra at low temperature were similar to the solution spectra, ReP1-NCXSQ established interactions with POPG producing a decrease in the protein unfolding temperature.

No changes in the spectral shape or in the dependence of the spectra with the temperature were observed in the presence of LUVs prepared with zwitterionic phosphatidylcholine lipids; the same spectra and temperature unfolding curves for the protein in solution were obtained both at 0.01 and 0.1 M NaCl (results not shown).

## CD spectroscopy

### *Temperature dependence of the interactions with DMPG and POPG LUVs*

Figure 3 shows representative spectra of ReP1-NCXSQ in DMPG and POPG LUVs in 0.01 M NaCl at different temperatures. At 20 °C we observed a relatively small increase in α-helix, larger in DMPG than in POPG. At 34 °C, when both lipids are in the liquid crystalline phase, we observed a large increase in the proportion of helix in DMPG. At 60 °C, the protein was unfolded in solution, but some secondary structure was conserved in both interfaces at this temperature. As a difference with FTIR, no diagnostic bands for self-aggregation are expected in the CD spectra. Visual inspection of the samples after heating up to 60 °C showed an evident macroscopic aggregation and precipitation. Then, the spectra in solution shown in Fig. 3c corresponded to an unfolded (i.e., with an increased amount of unordered structure) aggregated protein.

In the presence of anionic lipids, the temperature dependence of the spectra largely changed. Figure 3d shows the change in the spectral shape, measured by the ratio of ellipticities at 225 and 218 nm as a function of

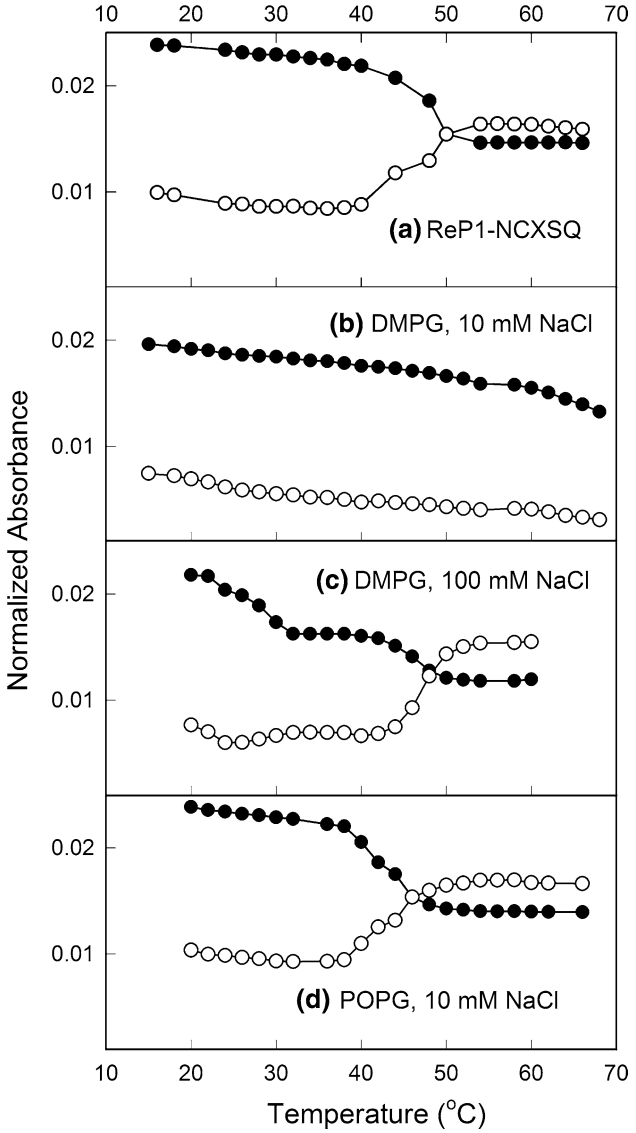


**Fig. 2** Infrared absorbance of ReP1-NCXSQ as a function of the temperature. The infrared absorbance of normalized spectra was measured at 1627 $cm^{-1}$ (*closed circle*) and at 1617 $cm^{-1}$ (*open circle*). Samples contained: **a** ReP1-NCXSQ in solution 0.01 M NaCl; **b** ReP1-NCXSQ with DMPG 0.01 M NaCl; **c** ReP1-NCXSQ with DMPG 0.1 M NaCl; **d** ReP1-NCXSQ with POPG 0.01 M NaCl. Concentrations were 130 μM protein and 13 mM lipid

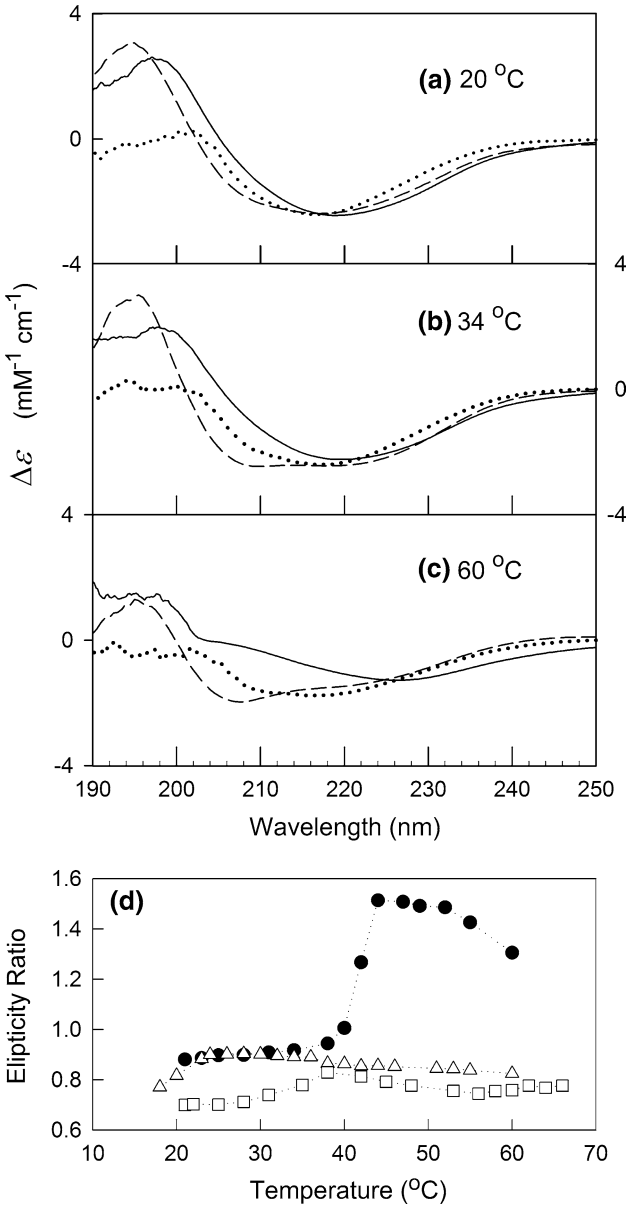


**Fig. 3** CD spectra of ReP1-NCXSQ at several temperatures. Comparison between protein in solution and in the presence of lipids. Spectra were taken at **a** 20 °C; **b** 34 °C; **c** 60 °C. *Continuous line* ReP1-NCXSQ in solution; *dashed line* ReP1-NCXSQ in the presence of DMPG; *dotted line* ReP1-NCXSQ in the presence of POPG. *Panel* **d** shows the ratio between the ellipticity at 225–218 nm as a function of the temperature. (*closed circle*) ReP1-NCXSQ in solution; (*triangle*) ReP1-NCXSQ with DMPG; (*square*) ReP1-NCXSQ with POPG. Concentrations were 10 μM protein and 1.3 mM lipid, 0.01 M NaCl

the temperature. Unfolding of the protein in solution was at 40–45 °C, few degrees below the unfolding observed in the FTIR experiments. In the presence of DMPG, a spectral change was observed within the range 18–25 °C without further changes as temperature increased. In the presence of POPG a transition, also of low amplitude as compared with the protein in solution, was observed in the range 30–40 °C. This transition, as also shown by FTIR spectroscopy in Fig. 2a, was at lower temperature than the protein in solution.

### *Interactions of Rep with LUVs and SUVs*

Figure 4 shows the CD spectra of ReP1-NCXSQ in solution and in the presence of DMPG, DPPG, POPG, DMPA, DMPS, and DMPC in the form of LUVs and SUVs. In

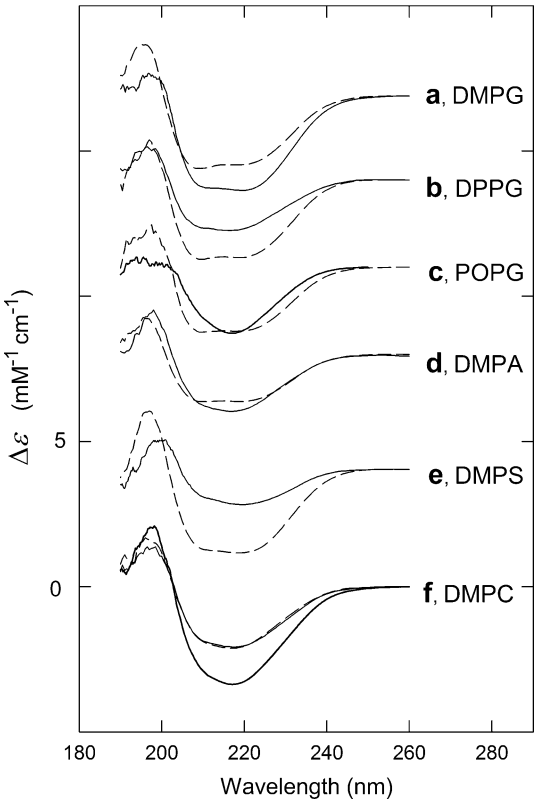


**Fig. 4** CD spectra of RePl-NCXSQ bound to lipid membranes. *Continuous line* RePl-NCXSQ bound to LUVs. *Dotted line* RePl-NCXSQ bound to SUVs. *Thicker line* together with the spectra in DMPC (*bottom spectra*): RePl-NCXSQ in solution. Temperature 29 °C, samples contained 10 μM protein, 2 mM lipid and 0.01 M NaCl. pH = 5.8

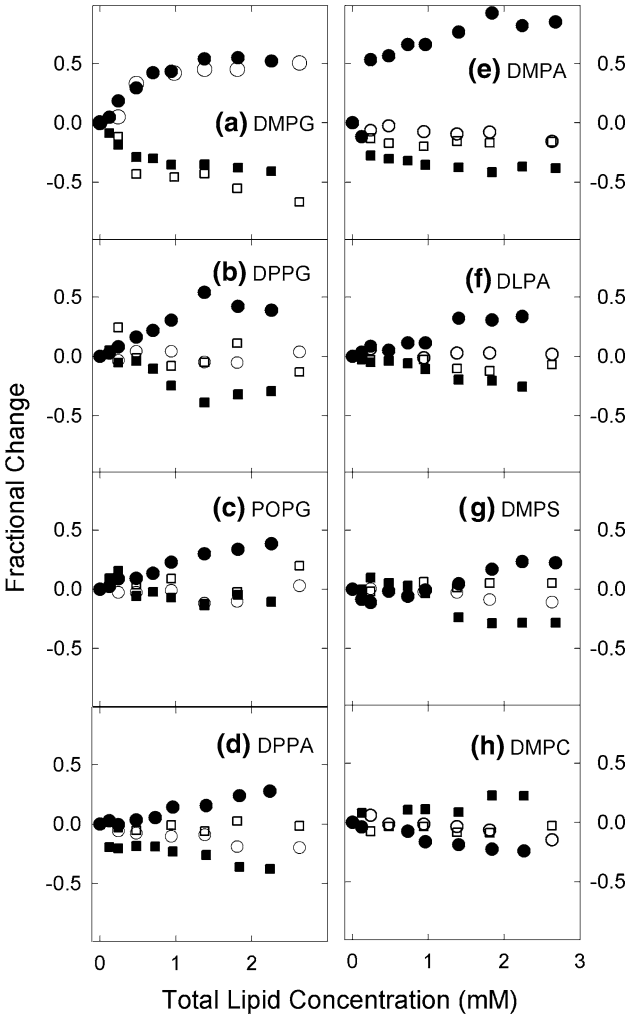


**Fig. 5** Fractional change of secondary structure of RePl-NCXSQ. *Circles* changes in α-helix; *squares* changes in β-strands; *filled symbols* in the presence of SUVs, *empty symbols* in the presence of LUVs. Samples contained 10 μM protein and 0.01 M NaCl. Temperature 29 °C, pH 5.8

solution, the CD spectrum corresponded to a protein with a large proportion of β-strands with a minimum at 216 nm. All the anionic phospholipids in the form of SUVs induced a change in the CD spectra of the membrane-bound protein corresponding to an increase in the α-helix proportion, this is the appearance of two minima at 210 and 222 nm. When the anionic lipids were in the form of LUVs, the spectral changes were smaller (continuous lines in Fig. 4). DMPG was an exception: it was equally efficient inducing an increase in α-helix both in the form of LUVs or SUVs. The zwitterionic lipid DMPC did not produce an appreciable change in the CD spectra of RePl-NCXSQ both as LUVs or SUVs. Using the CDPro package (see materials and methods) we obtained a proportion of 7% helix, 48% strands, 21% turns, and 24% unordered structure for the native protein in solution in the absence of lipid membranes. Figure 5 shows the changes in the proportion of α-helix an β-strands in Rep1-NCXSQ as a function of the lipid concentration. The numbers in Fig. 5 are fractional changes; this is the difference between the amount of secondary structure in the presence of lipid and the amount in the native protein divided by the amount in the native protein. Increasing amounts of lipids were added stepwise to the initially pure protein in solution. In the final samples, after addition of the maximum amount of lipid, we measured the membrane-bound protein using a filtration binding assay (see "Materials and methods"). About 70% of the protein was bound to the membranes of anionic lipids. No protein was bound to the zwitterionic DMPC. The spectra shown in Fig. 4 were obtained at the plateau regions in Fig. 5. Besides the lipids shown in Fig. 4, we also show the quantitative changes observed for dilauroylphosphatidic acid (DLPA) and dipalmitoylphosphatidic acid (DPPA). As already suggested by visual inspection of the spectra, we observed that, except for DMPG, all the studied anionic lipids induced a larger increase of α-helix when they

were in SUVs (filled circles) as compared to LUVs (empty circles). Actually, in most cases, anionic LUVs induced negligible changes in the structure of ReP1-NCXSQ. The quantitative analysis also sowed that DMPG was equally effective in inducing increase in α-helix both as SUVs or LUVs.

The experiments in Fig. 5 were performed at 29 °C. The gel to liquid-crystalline phase transition temperatures of DPPA and DPPG are 65 and 41 °C, respectively. Considering that above 40 °C, in solution, ReP1-NCXSQ is in the unfolded state, it was not possible to evaluate the capacity of these lipids in the liquid phase to induce α-helix. DLPA LUVs instead, with a phase transition at 31 °C, showed that both the gel (measurement at 29 °C) and the liquid-crystalline (measurement at 35 °C, not shown) were unable to induce a conformational change in ReP1-NCXSQ.

The results obtained with LUVs showed that the binding to anionic interfaces was not the only requisite to induce a conformational change in ReP1-NCXSQ. Clearly, DMPG extruded vesicles have a particular property, as compared to other anionic lipids, that induced the formation of non-native α-helix in ReP1-NCXSQ. Actually, DMPG has distinctive characteristics that place it apart from other phospholipids. The gel-to-liquid phase transition in DMPG occurs through an intermediate phase with remarkable properties like a decrease in turbidity, increase of viscosity, and electric conductivity (Schneider et al. 1999; Riske et al. 2009; Loew et al. 2011; Barroso et al. 2012; Enoki et al. 2012). It was proposed that the structure of this intermediate phase has a discontinuous "perforated" lateral organization. In the absence of added salts, the intermediate phase is largely populated between 17 and 35 °C, approximately. This temperature range decreases with an increase in ionic strength and spans between 19 and 30 °C at 10 mM ionic strength (Schneider et al. 1999; Riske et al. 2009). It is remarkable that the spectral change as a function of the temperature was in agreement with the temperature for the onset of the intermediate phase of DMPG (about 19 °C in 0.01 M NaCl, see Fig. 3d, triangles). The distinctive property of the intermediate phase, relevant to understand our results, is the presence of large pores or perforations (Riske et al. 2009; Loew et al. 2011; Barroso et al. 2012; Enoki et al. 2012). The border of the pores must be regions where the bilayer acquires a large curvature (see Fig. 10 in Riske et al. 2004). It can be postulated that this highly curved region has an increased affinity for the protein and can induce the formation of α-helix.

To some extent, SUVs mimic the region of high curvature already present in the extruded vesicles of DMPG. Figure 5 shows, as suggested qualitatively by the spectra in Fig. 4, that the anionic lipids unable to induce increases in the α-helix proportion of ReP1-NCXSQ in the form of LUVs induced conformational change when assembled in the form of SUVs.

## Discussion

In a previous work (Galassi et al. 2014) we showed, both by filtration binding assays and molecular dynamics simulations, that the binding to the anionic lipid POPG decreases with an increase in ionic strength and that the binding to the zwitterionic lipid phosphatidylcholine is largely reduced. These observations indicate that electrostatic interactions are required for the binding of ReP1-NCXSQ to lipid membranes. In this work, we found that binding to DMPG LUVs occurred with an increase in the amount of α-helix at the expense of β-strands. The conformational change was smaller when ReP1-NCXSQ was bound to LUVs of anionic lipids other that DMPG, suggesting that other interactions besides electrostatics are required for the conformational change. In the DMPG LUVs and low ionic strength condition, the FTIR spectra showed a large conformational change in the whole range of temperatures, suggesting a strong interaction with the membrane. Increasing the ionic strength to 0.1 M NaCl the spectral shape was similar to the native spectra in solution and self-aggregation also occurred at high temperatures. In this case, the dependence of the spectral shape with the temperature was similar to that observed for the fatty acid binding protein L-BABP in similar conditions (Decca et al. 2007, 2010). A transition in L-BABP at low temperatures occurred within the temperature range of the lipid phase transition. In that case, it was possible to observe the correlation between protein conformational changes and the lipid phase transition because the protein was globally unfolded only above 70 °C, allowing a suitable window in the temperature range: the conformational transition of L-BABP, coupled to the lipid phase transition, was observed at 24 °C in DMPG and at 50 °C in DPPG, in agreement with the lipid phase transition. ReP1-NCXSQ, instead, displayed a main transition at around 45 °C, which precluded the study of the eventual protein conformational changes coupled to the DPPG phase transition for example.

The FTIR experiments were done at a lipid-to-protein mole ratio at which increasing the lipid concentration produced no further changes in the spectra of the protein. Then, despite that we did not perform a rigorous measurement of binding constants at several temperatures, we can consider that the spectra corresponded to a membrane-bound protein.

Table 2 shows a comparison between the proportion of secondary structures of the native protein evaluated according to the crystallographic structure and the spectroscopic measurements. In our hands, the amount of α-helix was overestimated by FTIR and underestimated by CD spectroscopy. An apparent discrepancy was also observed for

**Table 2** Proportion of secondary structure components in native ReP1-NCXSQ

| | α-Helix | β-Strand | Turn | Bend | $3_{10}$-helix | Unassigned | Unordered |
|---|---|---|---|---|---|---|---|
| DSSP | 13 | 57 | 10 | 5 | 2 | 14 | |
| FTIR | 17 | 70 | 13 | | | | |
| CD | 7 | 48 | 21 | | | | 24 |

The proportions were calculated by the DSSP criteria, and band fitting to FTIR and CD spectra as described in the text. Numbers are % of the total amount of residues

DSSP criteria (Kabsch and Sander 1983), implemented in the program by Touw et al. (2015), http://swift.cmbi.ru.nl/gv/dssp/), was applied to the PDB entry ID 3PP6

the amount of β-strands, which is largely overestimated by FTIR. Nevertheless, it must be noted that no IR band was assigned to unordered structures according to our analysis of FSD and second derivative. Then, it is expected that the proportion of other bands must increase to compensate for the absence of this band. In the same way, several structures (like bend, $3_{10}$-helix and unassigned, in DSSP row in Table 2) are included under the "unordered" output from the CDpro analysis. Still, we consistently observed a much larger amount of β-strand as compared to α-helix.

The comparison between the results of FTIR and CD spectroscopy is not straightforward. It is remarkable that the conformational transition of the protein coupled to the lipid phase transition was observed in DMPG, at low ionic strength, in the CD but not in the FTIR experiments. In a CD experiment, the concentrations were typically 10 μM protein and 1 mM lipid while in the FTIR experiments they were in the range 100–200 μM protein and 10–20 mM lipid. Comparatively, the amount of aqueous phase is lower in a FTIR experiment and the binding equilibrium must be shifted toward the membrane-bound specie as compared with a CD experiment with the same total lipid-to-protein ratio. Probably, the main consequence of the large lipid concentration in the FTIR of experiments is to increase the crowding of components. Besides, considering the complexity of the phase transitions of DMPG, it is difficult to ascertain that the lipid is in the same state at a given temperature in the FTIR and CD samples.

Despite these differences, the same main conclusions were obtained with both methodologies. CD spectra clearly showed that ReP1-NCXSQ acquired α-helix secondary structure in the interaction with DMPG LUVs. The proportion of α-helix increased as a function of the temperature within the temperature range of the gel-to-intermediate phase transition. It must be noted that this was in a medium of low ionic strength. In the FTIR experiment, this dependence was observed when the binding was weaker; this is at higher ionic strength. Similarly to FTIR, CD revealed that the interactions with POPG LUVs was weaker: at low temperatures the spectra did not depart from the spectra of the protein in solution and no major increase in α-helix was observed. Still, ReP1-NCXSQ evidently interacted with POPG LUVs because in the FTIR experiments the transition in the protein occurred at lower temperature as compared to solution and the CD spectral changes observed at high temperature in solution were not observed in the presence of POPG.

The anionic lipids, unable to induce conformational change in the membrane-bound protein when assembled as LUVs, induced the formation of α-helix when they were assembled in structures of high curvature like the sonicated SUVs. This result is not unexpected, as the differential interaction of proteins with vesicles of different curvatures has been described in several systems (Nuscher et al. 2004; Chong et al. 2014). We postulate that the particular structure of DMPG in the intermediate phase, most probably the edges of pores induce the formation of α-helix.

A question remains about where, and driven by which forces, the increase of α-helix in the structure of ReP1-NCXSQ occurs. The acquisition of secondary structure of unfolded peptides in solution coupled to the binding to the lipid membrane has been well described within a solid thermodynamic background (Wimley and White 2004; Ladokhin and White 1999; Wimley et al. 1998; Klocek et al. 2009; Meier and Seelig 2007). Essentially, transferring a pair of polar groups from the solution to the lipid interface is energetically more favorable if they are linked by a hydrogen bond as compared to the transfer of the separate groups. Then, the membrane binding process is coupled to the increase in secondary structure, as it occurs with the formation of hydrogen bonds. Nevertheless, these studies demonstrate that the gain in free energy upon membrane binding is about the same for the formation of hydrogen bonds in an α-helix or between strands in the formation of parallel/antiparallel β-sheet. Then, we do not find a simple, straightforward, thermodynamic reason to explain why a helix structure should be preferred in the interface at the expense of β-strand. It is possible that subtle differences in the location within the membrane can make a difference for helix as compared to strand. Probably, the increase in α-helix in ReP1-NCXSQ is due to partial penetration into the membrane hydrophobic core, favored in regions of high curvature.

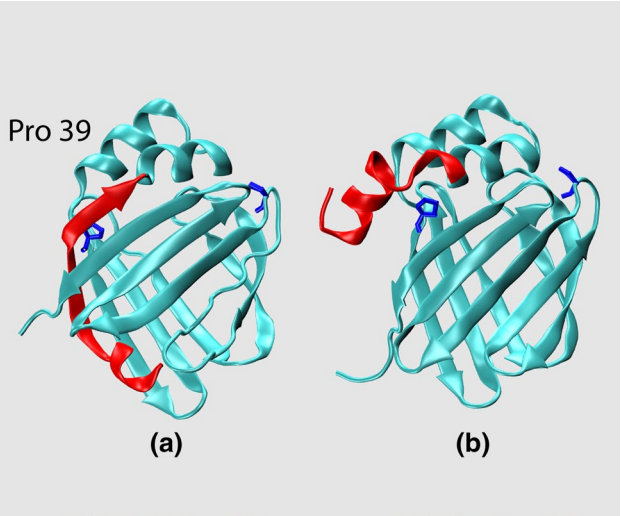


**Fig. 6** Structure of ReP1-NCXSQ. The 1–16 N terminal segment is shown in *red*. **a** The native structure (PDB ID: 3PP6, Cousido-Siah et al. 2012). **b** The 1–16 N terminal segment was drawn as α-helix. Proline residues are shown in *blue*

We suggest that the 1–16 N terminal segment (segment in red, Fig. 6a) is a good candidate to acquire α-helix structure in the membrane. It is more probable to extend a helix over an existing helix than starting a helix from a random or strand conformation. Following the sequence towards the C terminal, the helix hairpin in ReP1-NCXSQ finds a proline residue (Pro39, Fig. 6), which makes it unlikely to extend the α-helix in this direction. Taking the results of FTIR and CD together, the increase in α-helix was between 6 and 8% or about 8–10 residues for a protein with a total amount of 133 residues. This number is in agreement with the number of residues that would acquire helix structure in the N terminal segment. Just to show the possible structure, the 1–16 N terminal segment is shown as an α-helix in Fig. 6b.

According to our molecular dynamics simulations (Galassi et al. 2014), the first interactions of ReP1-NCXSQ with the anionic lipid membrane is through the α-helix hairpin domain, a result that is in agreement with the proposal of the propagation of the existing helix domains upon interaction with the interface.

Modulation of protein dynamics and conformation by the interaction with lipid interfaces determine the capacity of fatty acid-binding proteins to uptake and release ligands. These changes span a wide range of molecular motions, from mobility and compactness of side chains in the amino acids in the portal region, as demonstrated by Dyszy et al. (2013) in B-FABP, to large changes in the secondary structure as shown in the present work and in β-lactoglobulin (Zhang et al. 2007). Zhang et al. (2007) found that β-lactoglobulin increases its amount of α-helix secondary structure when interacting with anionic lipids, and that those changes depend on electrostatic and hydrophobic interactions. β-lactoglobulin is also a member of the lipocalin family with a structure similar to ReP1-NCXSQ: nine antiparallel β-strands, four short segments of $3_{10}$-helix, and a three-turn α-helix segment. It is suggestive that the N terminal of β-lactoglobulin does not have defined secondary structure (helix or β-strand) between Leu1 and Leu10 and a short $3_{10}$ helix segment span the residues Leu10-Ala16. This is a similar structural feature as in ReP1-NCXQ with similar possibilities for the N terminal segment to undergo a transition to helix structure.

It is interesting that the functions of ligand binding together with lipid membrane binding occur in proteins from different families and completely different structure. Micheletto et al. (2017) for example have shown that an ACBP, a four α-helix bundle protein, binds to lipid membranes depending on the electrostatic charge of the membrane. The membrane binding also occurs with a conformational change, in this case the loss of α-helix, and changes in the protein stability and ligand affinity.

The capacity of lipid membranes to modulate the aggregation of membrane-bound proteins attracts attention because of the interest in understanding the processes that drives polypeptides to an amyloid structure. Gorbenko and Trusova (2011) described that the physical basis for the aggregation of proteins within the lipid membrane environment are the local increase in protein concentration, the suitable orientation of adsorbed proteins (to undergo ordered aggregation) and the decreased activity of water in the interface. To the best of our knowledge, we present here the only case in which the lipid membrane inhibits the aggregation that otherwise should occur in solution. It seems to be a very particular case for ReP1-NCXSQ in DMPG at low ionic strength. It must be noted that a similar protein, L-BABP, does aggregate under similar conditions (Nolan et al. 2003; Decca et al. 2007, 2010). Considering that the initial interactions with the lipid membrane are through opposite domains, this is the bottom of the barrel in L-BABP (Villarreal et al. 2008) and the portal region in ReP1-NCXSQ (Galassi et al. 2014). It is possible that the final equilibrium orientations and membrane penetration were different, having an influence on the self-aggregation processes in the interface.

The final mechanism for the regulation of the $Na^+$/$Ca^{2+}$ transporter by ReP1-NCXSQ is still unknown. Several possibilities are proposed and discussed by Beaugé et al. (2013) including binding to the exchanger, perphosphorylation, removal of an inhibitory lipid, and allowing exchanger-activator interaction. Cousido-Siah et al. (2012) discovered that the capacity of ReP1-NCXSQ to bind the palmitic acid into the cavity is essential for the protein activity in the regulation of the transporter. The residue Tyr128 is directly related in the binding through H-bond to the polar

head group of the ligand. The mutant protein Tyr128Phe, incapable of establishing the mentioned H-bond, showed a decreased capacity both to retain the ligand and to activate the transporter (Cousido-Siah et al. 2012). Tyr128 is located in the middle of the β strand neighbor, antiparallel, to the N terminal β-strand that we propose as the segment that acquired α-helix structure when bound to the lipid membrane. Although very speculative, it can be proposed as a working hypothesis that the conformational change upon membrane interaction, or interaction with a macromolecular structure, can affect the conformation of the segment containing Tyr128 and consequently the affinity for the ligand. In this way, the membrane interaction and conformational change could be a mechanism to modulate the release of palmitic acid and the activation of the transporter.

## Conclusions

The interactions of the fatty acid-binding protein ReP1-NCXSQ with lipid membrane occurred with conformational changes of the protein, most noticeable an increase in α-helix and a reduction of β-strands. The extent of the conformational change was modulated by the strength of the interaction, depending on the ionic strength of the medium and the phase state of the lipid. In comparison to our previous studies about L-BABP, we conclude that the modulating effect of the phase state of the lipid could be a general mechanism of modulating protein conformation and not limited to a particular protein.

**Acknowledgements** We thank Dr. G. Berberián and Dr. L. Beaugé for the kind donation of cDNA for ReP1-NCXSQ. This work was supported by Consejo Nacional de Investigaciones Científicas y Técnicas, CONICET, Agencia Nacional de Promoción Científica y Tecnológica, AMPCyT, and Secretaría de Ciencia y Técnica-UNC, SECyT-UNC. CONICET also granted fellowships for VVG and SRS.

## References

Arrondo JL, Goñi FM (1999) Structure and dynamics of membrane proteins as studied by infrared spectroscopy. Prog Biophys Mol Biol 72:367–405

Barroso RP, Perez KR, Cuccovia IM, Lamy MT (2012) Aqueous dispersions of DMPG in low salt contain leaky vesicles. Chem Phys Lipids 65:169–177

Beaugé L, Dipolo R, Bollo M, Cousido A, Berberián G, Podjarny A (2013) Metabolic regulation of the squid nerve Na(+)/Ca (2+) exchanger: recent developments. Adv Exp Med Biol 961:149–161

Berberián G, Bollo M, Montich G, Roberts G, Degiorgis JA, DiPolo R, Beaugé L (2009) A novel lipid binding protein is a factor required for MgATP stimulation of the squid nerve Na+/Ca2+ exchanger. Biochim Biophys Acta 1788:1255–1262

Berberián G, Podjarny A, DiPolo R, Beaugé L (2012) Metabolic regulation of the squid nerve $Na^+/Ca^{2+}$ exchanger: recent kinetic, biochemical and structural developments. Prog Biophys Mol Biol 108:47–63

Berg OG, Gelb MH, Tsai MD, Jain MK (2001) Interfacial enzymology: the secreted phospholipase A2-paradigm. Chem Rev 9:2613–2654

Byler DM, Susi H (1986) Examination of the secondary structure of proteins by deconvolved FTIR spectra. Biopolymers 25:469–487

Casal HL, Mantsch HH (1984) Polymorphic phase behaviour of phospholipid membranes studied by infrared spectroscopy. Biochim Biophys Acta 779:381–401

Chong SSY, Taneva SG, Lee JMC, Cornell RB (2014) The curvature sensitivity of a membrane-binding amphipathic helix can be modulated by the charge on a flanking region. Biochemistry 53:450–461

Cornell RB, Ridgway ND (2015) CTP:phosphocholine cytidylyltransferase: function, regulation, and structure of an amphitropic enzyme required for membrane biogenesis. Prog Lipid Res 59:147–171

Cousido-Siah A, Ayoub D, Berberián G, Bollo M, Van Dorsselaer A, Debaene F, DiPolo R, Petrova T, Schulze-Briese C, Olieric V, Esteves A, Mitschler A, Sanglier-Cianférani S, Beaugé L, Podjarny A (2012) Structural and functional studies of ReP1-NCXSQ, a protein regulating the squid nerve Na+/Ca2+ exchanger. Acta Crystallogr D Biol Crystallogr 68:1098–1107

De Gerónimo E, Hagan RM, Wilton DC, Córsico B (2010) Natural ligand binding and transfer from liver fatty acid binding protein (LFABP) to membranes. Biochim Biophys Acta 1801:1082–1089

Decca MB, Perduca M, Monaco HL, Montich GG (2007) Conformational changes of chicken liver bile acid-binding protein bound to anionic lipid membrane are coupled to the lipid phase transitions. Biochim Biophys Acta 1768:1583–1591

Decca MB, Galassi VV, Perduca M, Monaco LH, Montich GG (2010) Influence of the lipid phase state and electrostatic surface potential on the conformations of a peripherally bound membrane protein. J Phys Chem B 46:15141–15150

Drake AF, Hider RC (1979) The structure of melittin in lipid bilayer membranes. Biochim Biophys Acta 555:371–373

Dyszy F, Pinto AP, Araújo AP, Costa-Filho AJ (2013) Probing the interaction of brain fatty acid binding protein (B-FABP) with model membranes. PLoS One 8:1–11

Enoki TA, Henriques VB, Lamy MT (2012) Light scattering on the structural characterization of DMPG vesicles along the bilayer anomalous phase transition. Chem Phys Lipids 165:826–837

Fanani ML, Hartel S, Maggio B, De Tullio L, Jara J, Olmos F, Oliveira RG (2010) The action of sphingomyelinase in lipid monolayers as revealed by microscopic image analysis. Biochim Biophys Acta 1798:1309–1323

Fidelio GD, Maggio B, Cumar FA (1982) Interaction of soluble and membrane proteins with monolayers of glycosphingolipids. Biochem J 203:717–725

Galassi VV, Villarreal MA, Posada V, Montich GG (2014) Interactions of the fatty acid-binding protein ReP1-NCXSQ with lipid membranes. Influence of the membrane electric field on binding and orientation. Biochim Biophys Acta 1838:910–920

Gorbenko G, Trusova V (2011) Protein aggregation in a membrane environment. Adv Protein Chem Struct Biol 84:113–142

Johnson WC (1999) Analyzing protein circular dichroism spectra for accurate secondary structures. Proteins: Struct Func Genet 35:307–312

Kabsch W, Sander C (1983) Dictionary of protein secondary structure: pattern recognition of hydrogen-bonded and geometrical features. Biopolymers 22:2577–2637

Klocek G, Schulthess T, Shai Y, Seelig J (2009) Thermodynamics of melittin binding to lipid bilayers. Aggregation and pore formation. Biochemistry 48:2586–2596

Ladokhin AS, White SH (1999) Folding of amphipathic alpha-helices on membranes: energetics of helix formation by melittin. J Mol Biol 285:1363–1369

Lefèvre T, Subirade M (2001) Conformational rearrangement of beta-lactoglobulin upon interaction with an anionic membrane. Biochim Biophys Acta 1549:37–50

Loew C, Riske KA, Lamy MT, Seelig J (2011) Thermal phase behavior of DMPG bilayers in aqueous dispersions as revealed by 2H- and 31P-NMR. Langmuir 27:10041–10049

Meier M, Seelig J (2007) Thermodynamics of the coil <==> beta-sheet transition in a membrane environment. J Mol Biol 369:277–289

Micheletto MC, Mendes LFS, Basso LGM, Fonseca-Maldonado RG, Costa-Filho AJ (2017) Lipid membranes and acyl-CoA esters promote opposing effects on acyl-CoA binding protein structure and stability. Int J Biol Macromol 102:284–296

Nolan V, Perduca M, Monaco HL, Maggio B, Montich GG (2003) Interactions of chicken liver basic fatty acid-binding protein with lipid membranes. Biochim Biophys Acta 1611:98–106

Nuscher B, Kamp F, Mehnert T, Odoy S, Haass C, Kahle PJ, Beyer K (2004) Alpha-synuclein has a high affinity for packing defects in a bilayer membrane: a thermodynamics study. J Biol Chem 279:21966–21975

Paolorossi M, Montich GG (2011) Conformational changes of β2-human glycoprotein I and lipid order in lipid-protein complexes. Biochim Biophys Acta 1808:2167–2177

Perrin RJ, Woods WS, Clayton DF, George JM (2000) Interaction of human alpha-Synuclein and Parkinson's disease variants with phospholipids. Structural analysis using site-directed mutagenesis. J Biol Chem 275:34393–34398

Provencher SW, Glöckner J (1981) Estimation of globular protein secondary structure from circular dichroism. Biochemistry 20:33–37

Raimunda D, Bollo M, Beaugé L, Berberián G (2009) Squid nerve $Na^+/Ca^{2+}$ exchanger expressed in *Saccharomyces cerevisiae*: up-regulation by a phosphorylated cytosolic protein (ReP1-NCXSQ) is identical to that of native exchanger in situ. Cell Calcium 45:499–508

Ramirez F, Jain MK (1991) Phospholipase A2 at the bilayer interface. Proteins 4:229–239

Rey-Burusco MF, Ibáñez-Shimabukuro M, Gabrielsen M, Franchini GR, Roe AJ, Griffiths K, Zhan B, Cooper A, Kennedy MW, Córsico B, Smith BO (2015) Diversity in the structures and ligand-binding sites of nematode fatty acid and retinol-binding proteins revealed by Na-FAR-1 from *Necator americanus*. Biochem J 471:403–414

Riske KA, Amaral LQ, Dobereiner HG, Lamy MT (2004) Mesoscopic structure in the chain-melting regime of anionic phospholipid vesicles: DMPG. Biophys J 86:3722–3733

Riske KA, Amaral LQ, Lamy MT (2009) Extensive bilayer perforation coupled with the phase transition region of an anionic phospholipid. Langmuir 25:10083–10091

Schneider MF, Marsh D, Jahn W, Kloesgen B, Heimburg T (1999) Network formation of lipid membranes: triggering structural transitions by chain melting. Proc Natl Acad Sci USA 25:14312–14317

Sreerama N, Woody RW (1993) A self-consistent method for the analysis of protein secondary structure from circular dichroism. Anal Biochem 209:32–44

Sreerama N, Venyaminov SY, Woody RW (2000) Estimation of protein secondary structure from circular dichroism spectra: inclusion of denatured proteins with native proteins in the analysis. Anal Biochem 287:243–251

Storch J, McDermott L (2009) Structural and functional analysis of fatty acid-binding proteins. J Lipid Res 50(Suppl):S126–S131

Surewicz WK, Leddy JJ, Mantsch HH (1990) Structure, stability, and receptor interaction of cholera toxin as studied by Fourier-transform infrared spectroscopy. Biochemistry 29:8106–8111

Touw WG, Baakman C, Black J, te Beek TAH, Krieger E, Robbie P, Vriend JG (2015) A series of PDB related databases for everyday needs. Nucleic Acids Research 43:D364–D368 **(database issue)**

Verger R (1997) 'Interfacial activation' of lipases: facts and artifacts. Trends Biotechnol 15:32–38

Villarreal MA, Perduca M, Monaco HL, Montich GG (2008) Binding and interactions of L-BABP to lipid membranes studied by molecular dynamic simulations. Biochim Biophys Acta 1778:1390–1397

Wang S-X, Sun Y-T, Sui S-F (2000) Membrane-induced conformational change in human apolipoprotein H. Biochem J 348:103–106

Wimley WC, White SH (2004) Reversible unfolding of beta-sheets in membranes: a calorimetric study. J Mol Biol 342:703–711

Wimley WC, Hristova K, Ladokhin AS, Silvestro L, Axelsen PH, White SH (1998) Folding of beta-sheet membrane proteins: a hydrophobic hexapeptide model. J Mol Biol 277:1091–1110

Wu JR, Lentz BR (1991) Fourier transform infrared spectroscopic study of $Ca^{2+}$ and membrane-induced secondary structural changes in bovine prothrombin and prothrombin fragment 1. Biophys J 60:70–80

Zhang X, Keiderling TA (2006) Lipid-induced conformational transitions of beta-lactoglobulin. Biochemistry 45:8444–8452

Zhang X, Ge N, Keiderling TA (2007) Electrostatic and hydrophobic interactions governing the interaction and binding of beta-lactoglobulin to membranes. Biochemistry 46:5252–5260